THRUSTER DYNAMICS COMPENSATION FOR THE POSITIONING OF UNDERWATER ROBOTIC VEHICLES THROUGH A FUZZY SLIDING MODE BASED APPROACH

Wallace Moreira Bessa
Federal Center for Technological Education – CEFET/RJ
Av. Maracanã, 229, 20271-110, Rio de Janeiro, RJ, Brazil
wmbessa@cefet-rj.br

Max Suell Dutra
Federal University of Rio de Janeiro – COPPE/PEM
PO Box 68503, 21945-970, Rio de Janeiro, RJ, Brazil
max@mecanica.coppe.ufrj.br

Edwin Kreuzer
Hamburg University of Technology – TUHH
Eissendorfer Strasse 42, D-21071, Hamburg, Germany
kreuzer@tuhh.de

Abstract. *The dynamic behavior of underwater robotic vehicles can be greatly influenced by the nonlinear dynamics of the vehicle thrusters. In this way, the implementation of a good control strategy for the thruster subsystem is essential for the accurate control of the entire robotic vehicle. It was already shown in the literature that without compensation for thruster dynamics the closed-loop positioning system can exhibit limit cycles. This undesired behavior may compromise the overall system stability and performance. This work focuses on the problem of controlling electrically actuated bladed thrusters, that are commonly employed in the dynamically positioning of remotely operated underwater vehicles. A sliding-mode compensator with fuzzy gain is proposed to stabilize the tracking error dynamics. Numerical simulation results suggest that this approach, when compared with an uncompensated counterpart, shows a greatly improved performance.*

Keywords: *Thruster Dynamics, Thrust Control, Sliding Modes, Fuzzy Logic and Underwater Robotic Vehicles.*

1. Introduction

The control system is one of the most important peaces of a Remotely Operated underwater Vehicle (ROV), and its characteristics (advantages and disadvantages) play an essential role when one have to choose a vehicle for a specific mission. These vehicles have been substituting the divers in the accomplishment of tasks that offer risks to the human life. In this way, ROVs have been used thoroughly in the research of sub phenomena and in assembly, inspection, and repair of offshore structures. During the execution of a certain task with the robotic vehicle, the operator needs to monitor and control a series of parameters. If some of these parameters, as for instance the position and attitude of the vehicle, could be attended automatically by a control system, the teleoperation of the ROV can be enormously facilitated.

A growing number of papers dedicated to problem of dynamic positioning of underwater robotic vehicles, confirms the necessity of the development of a controller, that could deal with the inherent nonlinear system dynamics, imprecise hydrodynamic coefficients and external disturbances. Many of these works (Bessa and Dutra, 2005; Whitcomb and Yoerger, 1999; Healey at al., 1995; Yoerger, Cooke and Slotine, 1990) addresses to the problem of the influence of thruster dynamics on overall vehicle behavior, and the importance of its incorporation into dynamic positioning system.

Traditionally, some thruster mathematical model is used directly to estimate, in a feed-forward manner, the required voltage (or current) to produce the desired thrust force. This strategy has as advantage the simplicity and the fact that it doesn't require the rotational velocity of the propeller to be measured. On the oder hand, it can only be used with a precise mathematical model of the thruster system. As shown in Bessa and Dutra (2005), the adoption of a standard model, available in the specialized literature, but not perfectly suited to the actual thrusters, is in many times the cause of the poor performance of ROV controllers. It was related in the literature (Yoerger, Cooke and Slotine, 1990) that this approach can lead to limit cycles in the closed-loop positioning system. As also related in Yoerger, Cooke and Slotine (1990) and confirmed in Bessa and Dutra (2005), this degradation in controller's performance is specially critical during low-speed maneuvering applications of the vehicle. In such cases, the dynamics of underwater robotic vehicles can be dominated by thruster dynamics.

An alternative approach that may be considered, specially when a precise mathematical model for the thruster system cannot be obtained, is the design of a feedback compensation subsystem for thruster dynamics. In this work, a sliding mode compensator with fuzzy gain is proposed to calculate the required voltage for each thruster. The choice of a variable gain, defined by a fuzzy inference system, makes the optimal trade-off between reaching time and tracking precision possible. The adoption of a saturation function (instead of a relay function) in controllers structure leads to a boundary layer, that can minimize or, when desired, even completely eliminate chattering. Using Barbalat's lemma the global stability of the closed-loop compensation subsystem and finite time convergence to the boundary layer was proven. Numerical simulations were carried out to demonstrate the robustness and improved performance of the compensation strategy.

2. Dynamic thruster model

The steady-state axial thrust (T) produced by marine thrusters is presented in the literature as proportional to the square of propeller's rotational velocity (Ω) (Newman, 1986). This quadratic relationship can be conveniently represented by

$$T = C_T\,\Omega|\Omega| \tag{1}$$

where C_T is a funcion of the advance ratio.

Taking the dynamical behavior of the thruster system into account, Yoerger, Cooke and Slotine (1990) presented a first order nonlinear dynamic thruster model with propeller's angular velocity as state variable. This dynamic model, that can be represented by Eq. (2) and Eq. (3), will be referred here as Model 1.

$$J_{msp}\dot{\Omega} + k_v\Omega|\Omega| = Q_m \tag{2}$$

$$T = C_T\,\Omega|\Omega| \tag{3}$$

where J_{msp} is the motor-shaft-propeller inertia and Q_m the input motor torque.

In posterior works (Bachmayer and Whitcomb, 2003; Healey at al., 1995; Fossen and Blanke, 1994), more accurate models employing lift and drag curves, and that also incorporates some other hydrodynamical effects, such as those caused by the rotational fluid velocity, were proposed. In all of these models, a second order dynamic system, with propeller's rotational velocity and axial fluid velocity as state variables, was used. However, during real operations with an underwater robotic vehicle, the axial fluid velocity cannot be measured with the required precision, which compromises its application for control purposes as a model state variable.

Nevertheless, if the following physically justified assumptions could be made:

1. Magnitude and direction of axial fluid velocity are mainly determined by propeller's rotational velocity,
2. Interference of the flow from one thruster to another is negligible,
3. Ambient fluid velocity and ROV's maneuvering speed are negligible, when compared with the axial fluid velocity generated by propeller's rotation,

the simplified first order dynamic model proposed by Yoerger, Cooke and Slotine (1990), Model 1, can satisfactorily be used as a part of the compensation strategy in robust control laws. The use of only propeller's rotational velocity (Ω) as state variable has as advantage the fact that it can be easily measured (or estimated) during real-time applications of the vehicle with sensors coupled to motor's shaft.

Based on experimental data, obtained from static tests (Bessa et al., 2004a) with the thruster unit of the AEGIR – *An Experimental General-purpose Internet-based underwater Robot* (Bessa et al., 2004b) – mounted in a wave channel, we propose a variation of Model 1 by incorporating some actuator's limitations, not considered in the original model. This modified version, that will be identied here as Model 2, can be mathematically represented by Equations (4)–(5):

$$J_{msp}\dot{\Omega} + k_{v1}\Omega + k_{v2}\Omega|\Omega| = \frac{k_t}{R_m}V_m \tag{4}$$

$$T = D(\Omega|\Omega|) \tag{5}$$

where V_m is the input voltage and $D(\Omega|\Omega|)$ represents a dead-zone nonlinearity with the quadratic input $\Omega|\Omega|$ and output T, as shown in Fig. (1), and that can be mathematically described by:

$$D(\Omega|\Omega|) = \begin{cases} k_l\,(\Omega|\Omega| - \delta_l) & \text{for} \quad \Omega|\Omega| \le \delta_l \\ 0 & \text{for} \quad \delta_l < \Omega|\Omega| < \delta_r \\ k_r\,(\Omega|\Omega| - \delta_r) & \text{for} \quad \Omega|\Omega| \ge \delta_r \end{cases}$$

The constants k_t and R_m, which represents the motor torque constant and winding resistance, respectively, can be obtained from motor's data-sheet. The values of k_{v1}, k_{v2}, k_l, k_r, δ_l and δ_r depends on constructive characteristics of

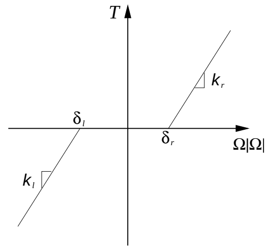

Figure 1. Dead-zone nonlinearity.

each thruster and must be experimentally determined. They will be here treated, in controller's design, as constants for each thruster unit. As will be shown, this simplification is acceptable due to the robustness of the proposed controller to parametric uncetainties.

By incorporating the term $k_{v1}\Omega$ in Eq. (4), Model 2 takes the back-emf torque and the viscous damping, due to mechanical sealing, into account. The term $k_{v2}\Omega|\Omega|$ represents the propeller rotational torque due to hydrodynamic loading. Through the adoption of Eq. (5) to describe the relationship between propeller's rotational velocity and thrust force, the modified model also considers friction losses during propeller's rotation. In the majority of works, the effect of friction losses is neglected.

The experimental data obtained in a wave channel with the thruster unit of the AEGIR, can be used to validate the proposed modifications to Model 1. Figure (2) shows some results from a comparative analysis between Model 1 (Yoerger, Cooke and Slotine, 1990), Model 2 (modified model), and experimental thruster's response. The required parameters for both models were obtained by an implementation of Levenberg–Marquadt's algorithm.

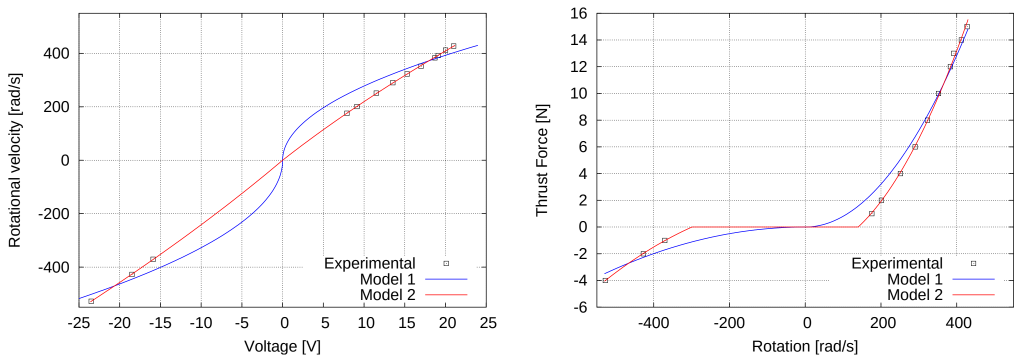

(a) Voltage × Rotational Velocity. (b) Rotational Velocity × Thrust force.

Figure 2. Obtained results for the comparative analysis between Model 1, Model 2 and experimental data.

As observed in Fig (2), Model 2 is better suited than Model 1 to represent thruster's response. This is due to the incorporation of some thruster's electro-mechanical characteristics and the effect of friction losses during propeller's rotation into the model. Such effects, that may be probably neglected in optimized thrusters, must be considered with the application of low-cost units.

3. Underwater robotic vehicle control

3.1 Vehicle model

An exact model to describe the underwater vehicle's dynamical behavior must include the rigid-body dynamics of the vehicle's body, the dynamics of the tether cable and a representation of the surrounding fluid dynamics. In this way, such a model must be composed by a system of ordinary differential equations, to represent rigid-body dynamics, and partial differential equations to represent both tether and fluid dynamics (*Navier–Stokes equation*).

To overcome the computational problem of solving a system with this degree of complexity, in the majority of works (Bessa and Dutra, 2005; Smallwood and Whitcomb, 2004; Hsu et al., 2000, Kiriazov, Kreuzer and Pinto, 1997) a lumped-parameters approach is employed to approximate vehicle's dynamical behavior.

In the range of velocities in which remotely operated underwater vehicles typically operate, never exceeding 2 m/s, the hydrodynamic forces (F_h) can be approximated using the *Morison equation* (Newman, 1986):

$$F_h = C_D \frac{1}{2} \rho A \dot{x} |\dot{x}| + C_M \rho \nabla \ddot{x} + \rho \nabla \dot{v}_w \tag{6}$$

where $\dot{x}$ and $\ddot{x}$ are, respectively, the relative velocity between the rigid-body and the fluid and the relative acceleration, $\dot{v}_w$ is the acceleration of underwater currents, A is a reference area, ρ is the fluid density, ∇ is the fluid's displaced volume, C_D and C_M are coefficients the must be experimentally obtained.

The last term of Eq. (6) is the so-called *Froude-Kryloff force* and will not be considered in this work due the fact, that at normal working depths, the acceleration of the underwater currents is negligible. In this way, the coefficient $C_M \rho \nabla$ of the second term will be called *hydrodynamical added mass*. The first term represents the nonlinear hydrodynamic quadratic damping. Experimental tests (Kleczka, Kreuzer and Pinto, 1992) shows that Morison equation describes with sufficient accuracy the hydrodynamic effects due relative motion between rigid-bodies and water.

In order to simplify the analysis of the thruster dynamic's influence onto the overall system behavior, we will adopt here a 1-DOF underwater vehicle model with exactly known parameters. Otherwise, the *actual* effect of thruster's dynamics over the vehicle's dynamics would be masquerade by some variable parameters and cross-coupling effects. The resulting dynamical model can be expressed by Eq. (7).

$$M \ddot{x} + C_D \frac{1}{2} \rho A \dot{x} |\dot{x}| = \tau \tag{7}$$

where τ is the total thrust force and M represents vehicle's mass plus the hydrodynamical added mass.

3.2 Vehicle controller

Based on the assumption of well-known parameters and to overtake the thruster dynamic's influence, we will adopt here a feedback-linearization approach for the dynamic positioning of the underwater robotic vehicle. The proposed control law can be written as

$$\tau_d = C_D \frac{1}{2} \rho A \dot{x} |\dot{x}| + M(\ddot{x}_d - 2\lambda \dot{\tilde{x}} - \lambda^2 \tilde{x}) \tag{8}$$

where x_d is the desired trajectory, $\tilde{x} = x - x_d$ is the tracking error and λ is a positive constant.

For this closed-loop system, composed by Eq. (7)–(8), we have the following error dynamics:

$$\ddot{\tilde{x}} + 2\lambda \dot{\tilde{x}} + \lambda^2 \tilde{x} = 0 \tag{9}$$

with coefficients that satisfies a Hurwitz polynomial, ensuring exponential convergence to zero.

Once we have, from Eq. (8), the required force to make the vehicle follow a prescribed trajectory, we can calculate the desired thrust force in each thruster by

$$T_d = \frac{\tau_d}{N_T} \tag{10}$$

where N_T is the available number of thrusters to actuate within the desired direction.

Finally, from Eq. (5), we can construct a dead-zone inverse to compute the desired propeller's angular velocity Ω_d.

4. Thruster Dynamics Compensation

Before starting with compensator's design, let us first rewrite the thruster's dynamical equation, Eq. (4), in a more conveniently way:

$$a \, \dot{\Omega} + b \, \Omega + c \, \Omega |\Omega| = u \tag{11}$$

where u is the input voltage and a, b and c are variable but positive and bounded parameters. If these parameters were perfectly known, then the following compensator would be enough to deal with thruster's dynamic:

$$u = b \, \Omega + c \, \Omega |\Omega| + a \, \dot{\Omega}_d \tag{12}$$

As is not case, because we only just have some estimates, $\hat{a}$, $\hat{b}$ and $\hat{c}$, of the parameters, let us treat the problem in a Filippov's way (Filippov, 1988), defining a law composed by an equivalent control $\hat{u} = \hat{b} \, \Omega + \hat{c} \, \Omega |\Omega| + \hat{a} \, \dot{\Omega}_d$ and a discontinuous term $-\mathcal{K}\text{sgn}(s)$, so that the resulting compensation law becomes:

$$u = \hat{b} \, \Omega + \hat{c} \, \Omega |\Omega| + \hat{a} \, \dot{\Omega}_d - \mathcal{K}\text{sgn}(s) \tag{13}$$

where $s = \tilde{\Omega} = \Omega - \Omega_d$, Ω_d is the desired propeller's angular velocity, $\mathcal{K}$ is the compensator's gain (which in this work will be variable and determined by a fuzzy inference system), and sgn$(\cdot)$ is defined by

$$\text{sgn}(z) = \begin{cases} -1 & \text{if} \quad z < 0 \\ 0 & \text{if} \quad z = 0 \\ 1 & \text{if} \quad z > 0 \end{cases}$$

The compensator established in Eq. (13) is based on the classical *sliding mode control* that originally appeared in Soviet literature (see Utkin, 1978). It's capable to deal with the parametric uncertainties but, as drawback, leads to high control activity and chattering. To overcome these limitations, the relay function sgn$(\cdot)$ in Eq. (13) can be replaced by a saturation function (Slotine and Li, 1991), defined as:

$$\text{sat}(z) = \begin{cases} \text{sgn}(z) & \text{if} \quad |z| \geq 1 \\ z & \text{if} \quad |z| < 1 \end{cases}$$

The substitution of sgn$(\cdot)$ by sat$(\cdot)$ leads to the appearance of a boundary layer (Φ) with designer's chosen width ϕ, which turn *perfect tracking* into a *tracking with guaranteed precision* problem.

To demonstrate the robustness of the proposed compensator to both structured and unstructured uncertainties, respectively parametric uncertainties and unmodeled dynamics, let us now define our compensation law based, not on the developed model (Model 2), but on some model picked from the literature, as for instance Model 1, which doesn't have the term $b\Omega$:

$$u = \hat{c}\,\Omega|\Omega| + \hat{a}\,\dot{\Omega}_d - \mathcal{K}\text{sat}\left(\frac{s}{\phi}\right) \tag{14}$$

Figure (3) shows the block diagram of the resulting vehicle's dynamic positioning system.

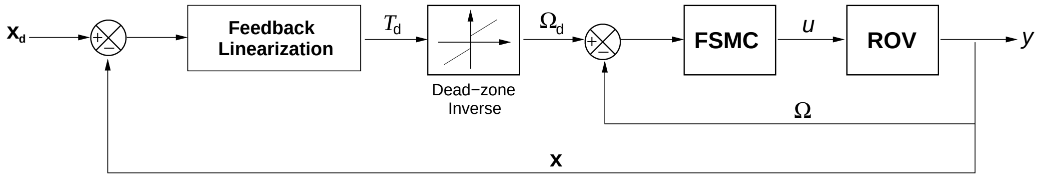

Figure 3. Block Diagram of the ROV controller with fuzzy sliding mode compensation for thruster dynamics.

The choice of a variable gain, defined by a fuzzy inference system, makes the optimal trade-off between reaching time and tracking precision possible. The adopted fuzzy inference system was the zero order TSK (Takagi–Sugeno–Kang), which rules can be stated in a linguistic manner, as follow:

If $|s|$ *is* S_n *then* $k_n = K_n \;\; ; \;\; n = 1, 2, \cdots, N$

where S_n are fuzzy sets represented by triangular and trapezoidal (at the extremes) membership functions, and K_n are chosen constants, with $K_n > K_{n-1}$.

Considering that each rule defines a constant numerical value as output k_n, the final output $\mathcal{K}$ can be computed by a weighted average:

$$\mathcal{K} = \frac{\sum_{n=1}^{N} w_n \cdot \, k_n}{\sum_{n=1}^{N} w_n} \tag{15}$$

where, for a rule base with N rules, w_n is the firing strength of each rule. As will be proved in Lemma 1, Equation (15) implies that $\mathcal{K}$ is bounded.

Lemma 1 *Let the Fuzzy Gain* $\mathcal{K}$ *be defined by Eq. (15), then* $\mathcal{K}$ *is bounded,* $K_{inf} \leq \mathcal{K} \leq K_{sup}$.

Proof: Equation (15) may be also written as $\mathcal{K} = K^{\mathrm{T}}\Psi(s)$, where, $K = [K_1, K_2, \ldots, K_N]$ is the vector with the values attributed to K_n, with $K_n > K_{n-1}$, for each rule, and $\Psi(s) = [\psi_1(s), \psi_2(s), \ldots, \psi_N(s)]$ is a vector with components: $\psi_n(s) = w_n / \sum_{n=1}^{N} w_n$. So, for the adopted membership functions (triangular at the middle and trapezoidal at the extremes), with the central values chosen as: $C = \{C_1 \; ; \; C_2 \; ; \; \ldots \; ; \; C_N\}$, we have for $s \leq C_1$, $\Psi(s) = [1, 0, \ldots, 0, 0]$, which implies $\mathcal{K} = K_1$. In the same way, for $s \geq C_N$ we have $\Psi(s) = [0, 0, \ldots, 0, 1]$, which implies $\mathcal{K} = K_N$, and completes the proof: $K_1 \leq \mathcal{K} \leq K_N$. □

Before proving the stability of the closed-loop system, let us first make the following physically motivated assumption:

Assumption 1 *The desired angular propeller's acceleration ($\dot{\Omega}_d$) is continuous, available and with known bounds.*

and recall Barbalat's lemma:

Lemma 2 (Barbalat) *If the differentiable function f has a finite limit as $t \to \infty$, and if $\dot{f}$ is uniformly continuous, then $\dot{f}(t) \to 0$ as $t \to \infty$.*

Proof: See Slotine and Li (1991). □

In addition to Barbalat's lemma, we can state that a sufficient condition for a differentiable function to be uniformly continuous is that its derivative be bounded.

The stability of the closed-loop system composed by Eq. (11) and Eq. (14) is established by the following theorem:

Theorem 1 *For the thruster system represented by Eq. (11), the sliding mode compensator defined in Eq. (14), with fuzzy gain $\mathcal{K}$ determined by Eq. (15), ensures global stability to the closed-loop system and finite time convergence to the boundary layer (Φ), for $\forall t \geq t_0$.*

Proof: To establish global boundedness of the closed-loop signals, let us first define a Lyapunov function candidate V, where

$$V(t) = \frac{1}{2} s_\phi^2 \tag{16}$$

and s_ϕ is a measure of the distance of the current state to the boundary layer (Φ), that can be defined as

$$s_\phi = s - \phi \,\mathrm{sat}(s/\phi) \tag{17}$$

Noting that $s_\phi = 0$ inside the boundary layer and $\dot{s_\phi} = \dot{s}$, we have $\dot{V}(t) = 0$ inside Φ, and outside:

$$\dot{V}(t) = s_\phi \dot{s}_\phi = s_\phi \dot{s} = (\dot{\Omega} - \dot{\Omega}_d) s_\phi = [a^{-1}(f+u) - \dot{\Omega}_d] s_\phi$$

where $u = -\hat{f} + \hat{a}\,\dot{\Omega}_d - \mathcal{K}\mathrm{sgn}(s)$ outside the boundary layer, $f = -b\,\Omega - c\,\Omega|\Omega|$ and $\hat{f} = -\hat{c}\,\Omega|\Omega|$. So, the time derivative of s takes the following form:

$$\dot{s} = a^{-1}[f - \hat{f} + \hat{a}\,\dot{\Omega} - \mathcal{K}\mathrm{sgn}(s)] - \dot{\Omega}_d \tag{18}$$

If the parameters a, b and c are unknown but assumed to be positive and bounded, which is physically coherent, and their estimates $\hat{a}$ and $\hat{c}$ are both positive constants, so that $|\hat{f} - f| \leq F$ and $\alpha^{-1} \leq \hat{a}/a \leq \alpha$, where $\alpha = \sqrt{a_{max}/a_{min}}$, then we have:

$$\begin{aligned}
\dot{V}(t) &= [a^{-1}(f+u) - \dot{\Omega}_d] s_\phi \\
&= \{a^{-1}[f - \hat{f} + \hat{a}\,\dot{\Omega}_d - \mathcal{K}\mathrm{sgn}(s)] - \dot{\Omega}_d\} s_\phi \\
&= -[a^{-1}(\hat{f} - f) + \dot{\Omega}_d - a^{-1}\hat{a}\,\dot{\Omega}_d + a^{-1}\mathcal{K}\mathrm{sgn}(s)] s_\phi
\end{aligned}$$

So, defining $\mathcal{K}$ as

$$\mathcal{K} \geq F + \alpha\eta + \hat{a}(\alpha - 1)|\dot{\Omega}_d|$$

we get:

$$\dot{V}(t) \leq -\frac{\eta}{\hat{a}} |s_\phi| \tag{19}$$

which implies that $V(t) \leq V(0)$, and therefore, that s_ϕ is bounded. From the definition of s_ϕ, Eq. (17), we can conclude that s is also bounded. Considering Eq. (18), Lemma 1 and Assumption 1, it can be verified that $\dot{s}$ is also bounded.

Finally, to establish the convergence properties of the system, we have to analyze the time derivative of $\dot{V}(t)$:

$$\ddot{V}(t) \leq -\frac{\eta}{\hat{a}} \frac{s_\phi}{|s_\phi|} \dot{s}$$

which implies that $\dot{V}(t)$ is bounded and, from Barbalat's lemma, that $s_\phi \to 0$ as $t \to \infty$. This ensures the global stability of the closed-loop system and finite time convergence to the boundary layer, completing the proof. □

In addition to Theorem 1, integrating both sides of Eq. (19), it can be easily verified that the boundary layer will be reached in a finite time smaller than

$$t_{reach} \leq \frac{\hat{a}\,|s_\phi(t=0)|}{\eta} \tag{20}$$

Theorem 1 also implies that the boundary layer is an invariant set, i.e., every system trajectory which starts from a point in Φ remains in Φ for $\forall t \geq 0$. Inside the boundary layer Φ, the error dynamics takes the following form:

$$a\dot{s} + \frac{\mathcal{K}}{\phi}s = \mathbf{p}\mathbf{y} \tag{21}$$

where $\mathbf{p} = [(\hat{a} - a)\,,\ -b\,,\ (\hat{c} - c)]^{\mathrm{T}}$ is the vector with parametric uncertainty, and $\mathbf{y} = [\dot{\Omega}_d\,,\ \Omega\,,\ \Omega|\Omega|]$.

5. Simulation Results

The simulation studies was performed with a numerical implementation, in C, with sampling rates of 500 Hz for ROV states and 1 kHz for propeller's rotational velocity. The chosen parameters for the ROV/thruster model, Eq. (5), (7) and (11) was: $k_r = k_l = 2.25 \times 10^4$, $\delta_r = -\delta_l = 5.75 \times 10^{-5}$, $M = 50$ kg, $A = 0.25$ m^2, $\rho = 1000$ kg/m^3 e $C_D = 1.2$ and $a(t) = 1.0 \times 10^{-2} \cdot \varepsilon(t)$, $b(t) = 4.0 \times 10^{-2} \cdot \varepsilon(t)$ and $c(t) = 1.4 \times 10^{-5} \cdot \varepsilon(t)$, with $\varepsilon(t) = 1 + 0.25\,\mathrm{sen}\,(|\Omega|t)$.

The performance of the proposed compensator, Eq. (14), was evaluated first in comparison with a conventional sliding mode compensator. The chosen parameters for the FSMC was $\hat{a} = 1.0 \times 10^{-2}$, $\hat{c} = 1.1 \times 10^{-4}$ and $\phi = 7.0$. For the fuzzy gain ($\mathcal{K}$) were adopted triangular and trapezoidal membership functions for S_n, with the central values defined as $C = \{7.0; 15.0; 25.0; 50.0; 100.0; 200.0; 400.0\}$ and associated crisp outputs $K_n = \{1.0; 1.5; 2.0; 3.0; 4.0; 6.0; 10.0\} \times K_{min}$, where $K_{min} = F + \alpha\eta + \hat{a}(\alpha - 1)|\dot{\Omega}_d|$, $F = 6.8$, $\alpha = 1.29$ and $\eta = 0.15$. For the conventional sliding mode controller we set $\mathcal{K}$ as constant, $\mathcal{K} = K_{min}$. Figure (4) shows some comparative results between FSMC and SMC.

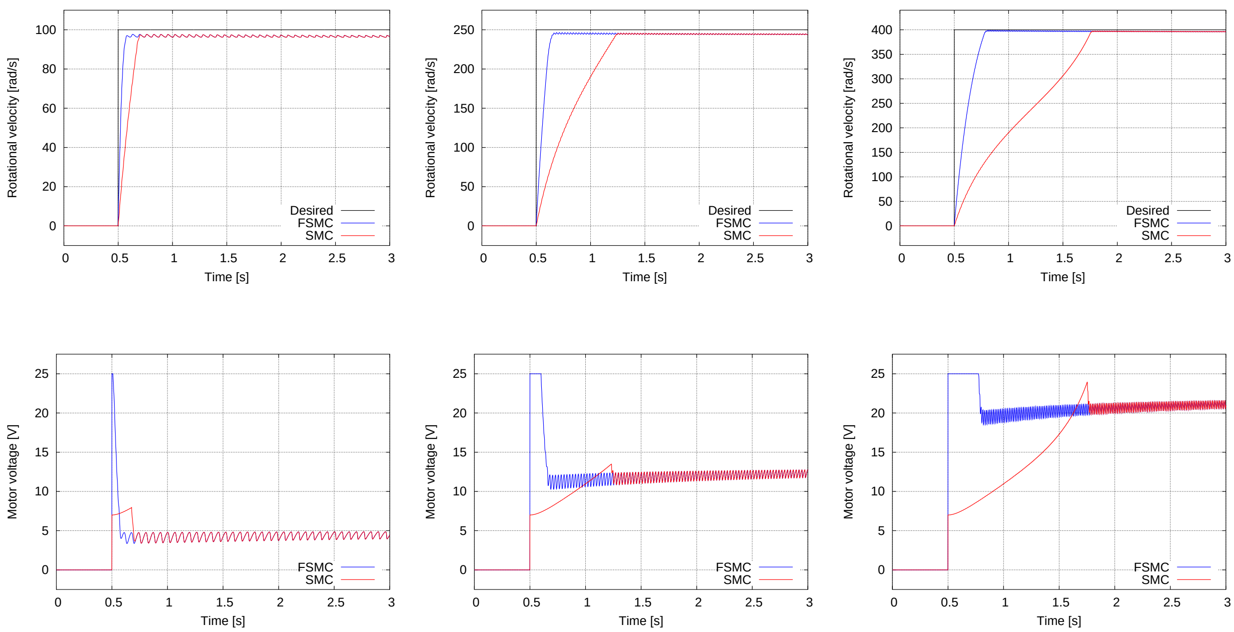

Figure 4. Propeller's rotational velocity (top) and the associated input voltage (bottom) for both fuzzy sliding mode compensator (FSMC) and conventional sliding mode compensator (SMC).

As observed in Fig (4), FSMC shows a better, and almost constant, rising time for different desired propeller's rotational velocities, without increasing control activity and chattering.

To demonstrate the improved performance of the ROV's dynamic positioning system with the FSMC, over the commonly adopted feed-forward approach, we show a comparison of both strategies in Fig. (5). In the feed-forward approach the input voltage was directly estimated, based on thruster's Model 2, with $u = \hat{b}\,\Omega_d + \hat{c}\,\Omega_d|\Omega_d|$, with $\hat{b} = 4.0 \times 10^{-2}$ and $\hat{c} = 1.4 \times 10^{-5}$. Note that despite the better suited parameters of this uncompensated strategy, the compensated counterpart shows a greatly improved performance.

6. Concluding Remarks

The present work considered the problem of compensating truster's dynamics in the dynamic positioning system of underwater robotic vehicles. A sliding-mode compensator with fuzzy gain is proposed to stabilize the tracking error dynamics. The global stability of the closed-loop compensation subsystem and the finite time convergence to the boundary layer was proven through a Lyapunov-like analysis based on Barbalat's lemma. Through numerical simulations, the im-

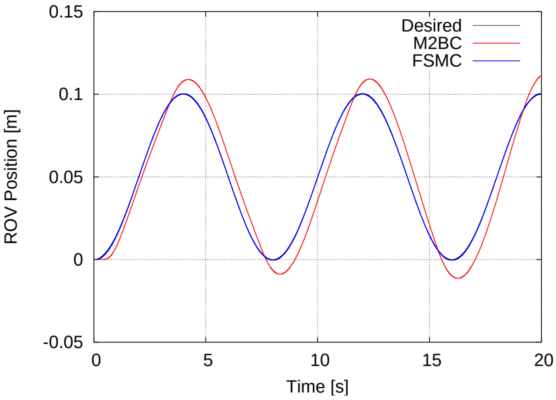

(a) Tracking in the time domain.

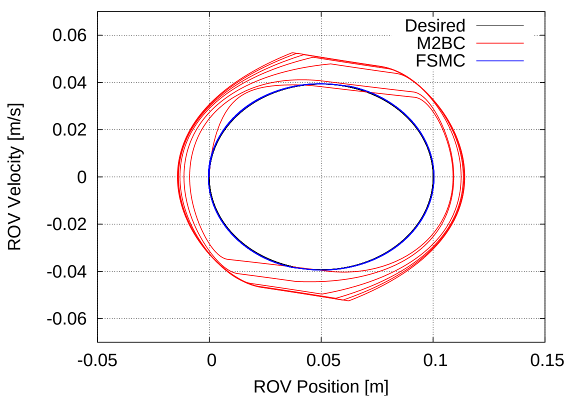

(b) Phase Portrait of the tracking.

Figure 5. Comparative analysis of the ROV positioning system with the proposed FSMC and with a feed-forward approach based on Model 2 (M2BC) for the tracking of $x_d = 0.05(1 - \cos(0.25\pi t))$ m.

proved performance and the robustness to both structured and unstructured uncertainties, namely parametric uncertainties and unmodeled dynamics, was demonstrated.

7. References

Bachmayer, R. and Whitcomb, L.L., 2003, "Adaptive Parameter Identification of an Accurate Nonlinear Dynamical Model for Marine Thrusters", ASME Journal of Dynamic Systems, Measurement, and Control, Vol.125, No.3, pp. 491–494.

Bessa, W.M. and Dutra, M.S., 2005, "Compensação da Dinâmica dos Propulsores no Controle de Posição de um Veículo Robótico Submarino", DINCON'2005, Proceedings of the 4th Thematic Congress on Dynamics, Control and Applications, Bauru, Brazil.

Bessa, W.M., Dutra, M.S., Kreuzer, E. and Salvi dos Reis, N.R., 2004, "Avaliação Experimental da Modelagem Matemática dos Propulsores de um Veículo Robótico Submarino", CONEM 2004, Proceedings of the 3rd National Congress of Mechanical Engineering, Belém, Brazil.

Bessa, W.M., Dutra, M.S., Kreuzer, E. and Salvi dos Reis, N.R., 2004, "Projeto e Construção de um Veículo Robótico Submarino Teleoperado via Internet", CONEM 2004, Proceedings of the 3rd National Congress of Mechanical Engineering, Belém, Brazil.

Filippov, A.F., 1988, Differential Equations with Discontinuous Right-hand Sides, Kluwer Academic, Dordrecht.

Fossen, T.I. and Blanke, M., 1994, "Nonlinear Output Feedback Control of Underwater Vehicle Propellere Using Feedback From Estimated Axial Flow Velocity", IEEE Journal of Oceanic Engineering, Vol.25, No.2, pp. 241–255.

Healey, A.J., Rock, S.M., Cody, S., Miles, D. and Brown, J.P., 1995, "Toward and Improved Understanding of Thruster Dynamics for Underwater Vehicles", IEEE Journal of Oceanic Engineering, Vol.20, No.4, pp. 354–361.

Hsu, L., Costa, R.R., Lizarralde, F. and Da Cunha, J.P.V.S, 2000, "Dynamic Positioning of Remotely Operated Underwater Vehicles", IEEE Robotics and Automation Magazine, Vol.7, No.3, pp. 21–31.

Kiriazov, P., Kreuzer, E. and Pinto, F.C., 1997, "Robust Feedback Stabilization of Underwater Robotic Vehicles", Robotics and Autonomous Systems, Vol.21, pp. 415–423.

Kleczka, W. Kreuzer, E. and Pinto, F.C., 1992, "Analytic-Numeric Study of a Submerged Double Pendulum", Internetional Symposium on Flow-Induced Vibration and Noise, Anaheim, USA.

Newman, J.N., 1986, "Marine Hydrodynamics", 5th Edition, MIT Press, Massachusetts.

Slotine, J.-J. E. and Li, W., 1991, "Applied Nonlinear Control", Prentice Hall, New Jersey.

Smallwood, D.A. and Whitcomb, L.L., 2004, "Model-Based Dynamic Positioning of Underwater Robotic Vehicles: Theory and Experiment", IEEE Journal of Oceanic Engineering, Vol.29, No.1.

Utkin, V.I., 1978, Sliding Modes and Their Application to Variable Structure Systems, MIR Publishers, Moscow.

Whitcomb, L.L. and Yoerger, D.R., 1999, "Preliminary Experiments in Model-Based Thruster Control for Underwater Vehicle Positioning", IEEE Journal of Oceanic Engineering, Vol.24, No.4, pp. 495–506.

Yoerger, D.R., Cooke, J.G. and Slotine, J.-J. E., 1990, "The Influence of Thruster Dynamics on Underwater Vehicle Behavior and their Incorporation into Control System Design", IEEE Journal of Oceanic Engineering, Vol.15, No.3, pp. 167–178.